

## 14.5 IMPROVED SPATIAL MONITORING OF AIR TEMPERATURE IN FORESTED COMPLEX TERRAIN: AN ENERGY-BALANCE BASED CALIBRATION METHOD

Adam M. Kennedy\*, Christoph K. Thomas, John S. Selker, Mike H. Unsworth  
Oregon State University, Corvallis, Oregon

### 1 INTRODUCTION

Fiber-optic distributed temperature sensing (DTS) systems have great potential for spatial monitoring in atmospheric boundary layer applications and hydrology (Sayde et al., 2010; Roth et al., 2010; Petrides et al., In Review). These novel systems have an advantage over arrays of conventional individual temperature sensors in that thousands of quasi-concurrent temperature measurements may be made at 1 m increments along the entire length of a fiber several thousands of meters long by a single instrument, thus increasing measurement precision and spatial coverage substantially. However, basic research has documented the importance of deploying temperature sensors within radiation shields to reduce the amount of radiation error in the reported temperature measurement (Fuchs and Tanner, 1965; Nakamura and Mahrt, 2005).

In our case, a fiber optic temperature sensing cable has no radiation shield and the fiber temperature is influenced by energy exchange with its environment, particularly by radiant energy (short and longwave) and modulated by wind speed. As mean wind speed increases, the resistance to convective heat transfer of a cylinder (the fiber in this case) exposed to that wind decreases, increasing the sensible heat flux and decreasing the temperature difference between the fiber and the air. When evaluating the behavior between individual black and white fibers, an increase in mean wind speed across fibers decreases the resistance to sensible heat transfer, and assuming constant incoming short and longwave radiation, will, as the system reaches equilibrium, decrease the temperature difference between the fibers. It is our aim to use an energy balance based approach to correct for radiation and wind influences on fiber deployed in the atmosphere in order to obtain accurate and spatially distributed temperature measurements.

The objective of this study is to quantify the en-

ergy excess between a white fiber and an air temperature reference, a black fiber and an air temperature reference, and between a white and black fiber in a controlled wind tunnel experiment. Ultimately, our goal is to develop a physical model of the energy balance of the DTS fibers, which can then be applied to compute the true air temperature for measurements in open and forested environments.

### 2 METHODOLOGY

#### 2.1 Distributed Temperature Sensing (DTS)

To obtain temperature measurements from a fiber optic cable, laser pulses from the DTS controller are sent along the glass fiber inside the fiber housing. As these pulses travel through imperfections in the glass fiber, light is back-scattered in small bursts of slightly shifted frequencies to the beginning of the fiber that is connected to the controller. This determines the relative temperature of the fiber section from which the back-scattered pulse of light originated. Since the velocity of light is constant, the round-trip travel time of the laser pulse to the controller determines the position of the recorded temperature along the fiber (Smolen and van der Spek, 2003; Selker et al., 2006). The relative temperature reported by the controller is then referenced to air temperature references, ice bath, and other calibration points to obtain an accurate temperature of the fiber section.

#### 2.2 Fiber Calibration in the Dark

To characterize the fiber temperature measurement in air across a wide temperature range, a dark calibration chamber was constructed to compare the temperatures reported by the fiber to that of an air temperature reference. Twenty meters of twisted black and white fiber were loosely wound around a 30 cm by 7 cm diameter mesh tube. The space within the tube housed one platinum resistance thermometer (Omega, part# EI1502112-RTD-810-3-36" with the linearizer Omega, part# OM5-IP4-100-C) and two additional

---

\*Corresponding author: Adam M. Kennedy, College of Oceanic and Atmospheric Sciences, Biomicroeteorology Group, Oregon State University, 104 COAS Admin Bldg, Corvallis, OR 97331, USA; Email: akennedy@coas.oregonstate.edu

temperature sensors (Vaisala Inc. HMP45C). This instrumented mesh tube was fitted inside a ventilated 0.1 m by 3.0 m white PVC tube. Both fibers were routed through an ice bath held constant at 0°C and an aerated span water bath that fluctuated with ambient temperature so that the total deployment featured two ice bath sections, a span reference section, and an air reference section (Figure 1).

## 2.3 Post-processing Correction Models Applied to Fiber Data in the Dark

Following the internal configuration of the DTS controller (SensorNet ORYX) with SensorNet software (v.3.7.1.2), additional post-processing procedures with both the loosely coiled fiber and wind tunnel deployed fiber (see later) were performed on the raw traces to obtain an accurate fiber air temperature measurement during conditions when neither the air reference nor fiber was exposed to direct shortwave radiation. Three correction models were used to correct for differentials between the fiber and a temperature reference.

### 2.3.1 Constant Offset Model (M1A)

To correct the constant temperature offset between the section of the fiber in the ice bath and an ice bath temperature reference, the difference between the ice bath reference and the fiber ice bath section average was added to the observed temperature along the entire length of the fiber (Eq. 1).

Model M1A may be written

$$T_{oc} = T_f + (T_{ir} - T_{fir}) \quad (1)$$

where  $T_{oc}$  is the temperature offset corrected fiber observation,  $T_f$  is the raw fiber temperature,  $T_{ir}$  is the ice bath temperature reference, and  $T_{fir}$  is the average temperature of the fiber ice reference section (after verifying that the temperature difference between the first and second ice bath sections was zero).

### 2.3.2 A Correction Model for the Mean Linear Differential (M2A)

In an optimal deployment scenario, a span bath is incorporated into the initial fiber configuration. This span bath permits an independent calibration model to be constructed that uses a span reference temperature and a span fiber reference section. When a span bath is incorporated into the calibration procedure, it is

possible to construct a mean linear model in the form  $\mu\{T_{oc}|T_{sar}\} = \beta_0 + \beta_1 T_{sar}$ , where  $\mu\{T_{oc}|T_{sar}\}$  is read as the mean of  $T_{oc}$  as a function of  $T_{sar}$ ,  $\beta_0$  is the intercept of the line, and  $\beta_1$  is the slope of the line and  $T_{sar}$  is the reference temperature of the span bath. The mean linear differential correction coefficients ( $\beta_0$  and  $\beta_1$ ) determined from this model are then used to correct the  $T_{oc}$  observations along the entire airborne section of the fiber over the entire range of  $T_{oc}$  (Eq. 2).

Model M2A may be written

$$T_{fcm} = T_{oc} - (\beta_1 T_{oc} + \beta_0) \quad (2)$$

where  $T_{fcm}$  is the final corrected fiber temperature measurement derived from the M2A model.

### 2.3.3 Single Point in Time and Space Correction Model (M2B)

If a span bath reference is not used during a fiber deployment, a simpler correction method may be applied to correct for the linear differential between  $T_{oc}$  and the reference air temperature ( $T_{ar}$ ) over the entire range of  $T_{ar}$ . The single point in space and time correction model (M2B) coefficient is constructed from the ratio of  $T_{arp} T_{ocp}^{-1}$ , where  $T_{arp}$  and  $T_{ocp}$  are  $T_{ar}$  and  $T_{oc}$  at a single point in time and space respectively during conditions when the temperature difference between a fiber section (or point) and the co-located air reference should be zero (Eq. 3).

Model M2B may be written

$$T_{fcs} = \frac{T_{arp}}{T_{ocp}} * T_{oc} \quad (3)$$

where  $T_{fcs}$  is the fiber temperature final correction using a single point in time and space calibration model.

## 2.4 Wind Tunnel Setup and Design

To better understand the physics controlling the fiber temperature reported by the controller, alternating black and white fiber-optic cables were installed on vertical wooden jigs inside a recirculating wind tunnel. The fibers were laced through the jig to form an alternating black and white vertical web of fiber. A constant irradiance from six 600 W halogen lamps was directed

on a one meter square area of fiber to permit controlled observations of the resulting temperature difference between the black and white fibers and a temperature reference as wind speed was varied (Figure 2). Inside the tunnel, net short and longwave radiation balance of each fiber was measured with an Eppley (Model PSP) pyranometer and Kipp and Zonen (CGR 4) pyrgeometer, air temperature was measured with a PT-1000 platinum resistance thermometer (Campbell Scientific 43347 RTD Temperature Probe ( $\pm 0.1^\circ C$ )) mounted in a fan aspirated radiation shield, sonic anemometers (Gill WindSonic) were positioned to record wind speed and turbulence. Outside the tunnel in the ice reference bath, a PT-100 platinum resistance temperature sensor (Omega, part# EI1502112-RTD-810-3-36") with the linearizer (Omega, part# OM5-IP4-100-C), which was calibrated by the Ameriflux QA/QC lab using the triple point of water,  $0^\circ C$ , the melting point of Gallium,  $26.771^\circ C$ , and the boiling point of water,  $100^\circ C$  (AmeriFlux QA/QC [viewed online: 2010]). The PT-100 was co-located with the fiber ice reference sections.

## 2.5 Energy Balance Calibration Model

Wind and radiation loads on fiber deployed in atmospheric conditions require radiation and wind speed corrections in order to obtain an accurate air temperature, otherwise, the temperature of the fiber will be reported and with it the associated excess energy from radiation exposure. Thus, the goal of the energy balance calibration is to robustly quantify the excess energy responsible for the temperature differential between the observed black and white fiber and reference air temperature by i) computing the radiation balance of each fiber (Eq. 4), ii) applying energy balance coefficients to account for wind and radiation to predict the actual air temperature from corrected fiber measurements (Eq. 5), and iii) use the net radiation difference between the black and white fiber to quantify, in addition to actual air temperature, distributed solar radiation across the landscape (Eq. 7).

The energy balance of a fiber may be written

$$R_{n(b,w)} = \varepsilon_{b,w}L_i - \varepsilon_{b,w}\sigma T_{fc(b,w)}^4 + (1 - \alpha_{b,w})S_i \quad (4)$$

where  $R_n$  is net radiation of a black or white fiber,  $T_{fc}$  is the corrected temperature of a fiber,  $L_i$  and  $S_i$  represent incoming long and short wave radiation respectively, and  $\sigma$  is the Stephan-Boltzman Constant.

Both the albedo ( $\alpha$ ) and emissivity ( $\varepsilon$ ) are measurable properties of a cylindrical fiber. Here, model coefficients are subscripted with a "b" or "w" to distinguish between the black or white fiber.

Assuming that  $R_n$  is balanced by convective heat loss,

$$\Delta T_{fr} \propto \frac{r_H}{\rho C_p} R_{n(w)} \quad (5)$$

where  $\Delta T_{fr} = (T_{fc(w)} - T_{ar})$ ,  $r_H$  is the resistance to heat transfer of the fiber (related to wind speed by Nusselt and Reynolds numbers),  $\rho$  is the density of air,  $C_p$  is the specific heat of air, and  $R_{n(w)}$  is the net radiation of the fiber.

The difference in  $R_n$  between the black and white fiber may be written

$$S_i = \frac{\Delta T_f \left( \frac{\rho C_p}{r_H} - 4\sigma T_b^3 (\varepsilon_b - \Delta\varepsilon) \right) - \Delta\varepsilon (L_i + \sigma T_b^4)}{(\alpha_w - \alpha_b)} \quad (6)$$

where  $S_i$  is the incoming shortwave radiation at 1 m increments (or DTS specific minimum spatial resolution),  $\Delta T_f = T_{fc(b)} - T_{fc(w)}$ ,  $\varepsilon_b$  is the emissivity of the black fiber,  $\Delta\varepsilon(\alpha)$  is the emissivity (albedo) difference between the black and white fiber, and  $L_i$  is the incoming longwave radiation.

If  $\Delta\varepsilon$  is very small, equation 6 can be simplified to

$$S_i = \frac{\Delta T_f \left( \frac{\rho C_p}{r_H} - 4\varepsilon_b \sigma T_b^3 \right)}{(\alpha_w - \alpha_b)} \quad (7)$$

## 3 RESULTS

Following post-processing correction routines, both the constant offset and linear differential models were able to minimize the difference between  $T_{fc(b,w)}$  and  $T_{ar}$  in the following ways: 1) the dark chamber fiber data were corrected with model M2A because the fiber was routed through a referenced span bath and 2) the wind tunnel data were corrected with model M2B, because no reference span bath was used. Instead, model M2B coefficients were computed when the tunnel was dark. After all post-processing was completed, the wind tunnel results of the temperature differences between  $T_{fc(b)}$  and  $T_{fc(w)}$  and between  $T_{fc(w)}$  and  $T_{ar}$  indicate 1) the temperature difference between  $T_{fc(b,w)}$  and  $T_{ar}$  and between  $T_{fc(b)}$  and  $T_{fc(w)}$  increases with increasing radiation and decreases with

increasing wind speed as expected and 2) the temperature difference between an aspirated, radiation-shielded thermometer ( $T_{ar}$ ) and a white fiber ( $T_{fc(w)}$ ) may be several degrees in typical canopy shaded conditions where the shortwave radiation is between 5 and 20% of shortwave radiation above the canopy despite the small diameter of the fiber (0.9 mm) and even greater for a black fiber of identical dimensions (most notably at mean wind speeds less than  $0.4 \text{ m s}^{-1}$ ). Temperature differences between the black and white fibers ranged from  $0.7$  to  $3.1^\circ\text{C}$ , between black and air reference from  $1.2$  to  $10.0^\circ\text{C}$ , and between white and air reference  $0.1$  to  $8.0^\circ\text{C}$  over the shortwave radiation fields ( $246$  to  $404 \text{ W m}^{-2}$ ) and wind speeds ( $0.2$  -  $3.0 \text{ m s}^{-1}$ ) examined (Figure 3). Additional analysis of the energy balance calibration approach is in progress.

#### 4 SUMMARY

These results obtained during controlled laboratory wind tunnel experiments characterize the fiber response to levels of radiation and wind that we would expect if it were deployed under typical canopy conditions. The correction methods will be applied in upcoming field trials at an extensively monitored level field site, and later across steep and complex terrain with varying levels of canopy closure to better characterize air flow and temperature fields. Because of promising results observed during these experiments, it is reasonable to suggest that an energy balance approach is a practical correction technique for airborne deployments of temperature sensing fiber across a landscape. However, thorough post-processing that considers both radiation and mean wind speed (in addition to differential artifacts introduced by the DTS instrumentation itself) is required to derive an actual air temperature from the temperature measurement of the fiber.

Distributed temperature sensing has great potential in atmospheric and other environmental sciences but basic wind and radiation influences must first be understood before the resulting data will see its full potential in scientific applications. DTS observations should encourage the visualization of spatial temperature fields in complex terrain and facilitate the computation of advective transport of sensible heat on micro to mesoscales and how these fields communicate across the landscape.

#### References

- Fuchs, M. and C. B. Tanner, 1965: Radiation shields for air temperature thermometers. *Journal of Applied Meteorology*, **4**, 544–547.
- Nakamura, R. and L. Mahrt, 2005: Air temperature measurement errors in naturally ventilated radiation shields. *Journal of Atmospheric and Oceanic Technology*, **22**, 1046–1058.
- Petrides, A., J. Gabrielli, A. Arik, N. V. de Giesen, A. M. Kennedy, C. K. Thomas, and J. S. Selker, In Review: Distributed stream shade monitoring. *Water Resources Research*.
- Roth, T. R., et al., 2010: Stream temperature response to three riparian vegetation scenarios by use of a distributed temperature validated model. *Environ. Sci. Technol.*, **44** (6), 2072–2078, doi:10.1021/es902654f.
- Sayde, C., C. Gregory, M. Gil-Rodriguez, N. Tufillaro, S. Tyler, N. van de Giesen, M. English, and R. C. J. S. Selker, 2010: Feasibility of soil moisture monitoring with heated fiber optics. *Water Resources Research*, (46), doi:10.1029/2009WR007846.
- Selker, J. S., et al., 2006: Distributed fiber-optic temperature sensing for hydrologic systems. *Water Resources Research*, **42** (W12202), 1–8, doi:10.1029/2006WR005326.
- Smolen, J. J. and A. van der Spek, 2003: *Distributed temperature sensing: A DTS primer for oil and gas production*.
- Acknowledgments. The author gratefully acknowledges useful discussions and suggestions with Barbara Bond and Nick van de Giesen. I also wish to acknowledge Chris Gregory, Travis Roth, Julie Huff, Aida Arik for technical assistance, and James Liburdy for generously providing wind tunnel facilities during this experiment. This material is based upon work supported by Grant DBI-0529223 titled SIRG: A Wireless Network of Battery-Free Sensors for Atmosphere-Biosphere Studies in Complex Environments from the National Science Foundation.

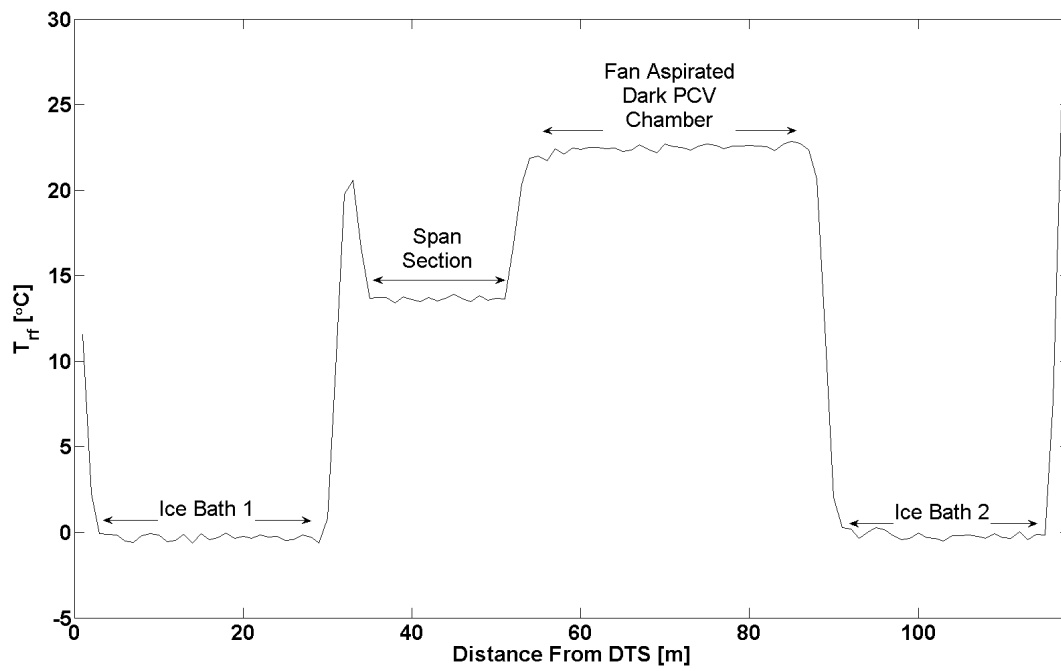


Figure 1: Layout of fiber used in dark calibration experiments.



Figure 2: Fiber and instrumentation configuration inside wind tunnel.

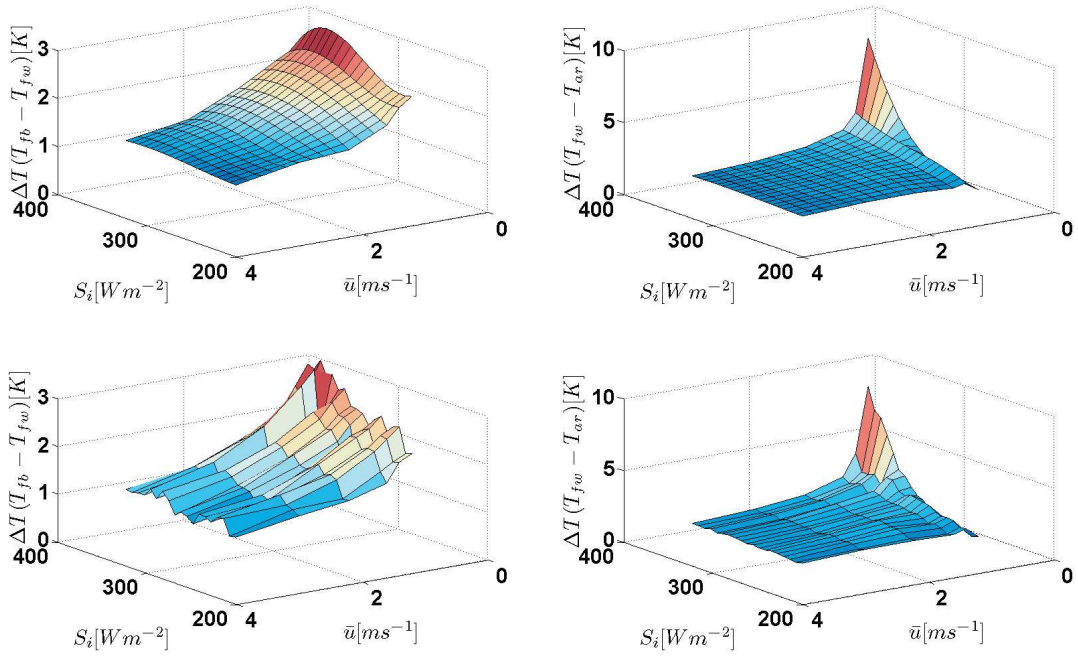


Figure 3: Modeled (upper) and actual (lower) temperature differences between black ( $T_{fb}$ ) and white ( $T_{fw}$ ) fibers and air temperature reference ( $T_{ar}$ ) during the wind tunnel trials over both wind ( $\bar{u}$ ) and shortwave radiation ( $S_i$ ) gradients.